Ordered assembling of Co tetra phenyl porphyrin on oxygen-passivated Fe(001): from single to multilayer films

Alberto Calloni[1,*], *Madan* S. Jagadeesh[1], *Guglielmo* Albani[1], *Claudio* Goletti[2], *Lamberto* Duò[1], *Franco* Ciccacci[1], *Gianlorenzo* Bussetti[1]

[1]Dipartimento di Fisica, Politecnico di Milano, piazza Leonardo da Vinci 32, Milano I-20133, Italy
[2]Dipartimento di Fisica, Università di Roma 'Tor Vergata', via di Tor Vergata, 00133 Roma, Italy

Abstract. Tetra-phenyl prophyrins (TPP) are an interesting class of organic molecules characterized by a ring structure with a metal ion in their centre. An ordered growth of such molecules can be obtained even on metallic substrates by means of a proper modification of the reactive interface, as we demonstrated for ZnTPP molecules coupled to oxygen-passivated Fe(001) [G. Bussetti *et al.* Appl. Surf. Sci. **390**, 856 (2016)]. More recently, we focused on CoTPP molecules, characterized by a not nil magnetic moment and therefore of potential interest for magnetic applications. As in the ZnTPP case, our results for one monolayer coverage report the formation of an ordered assembly of flat-lying molecules. However, some differences between the two molecular species are observed in the packing scheme and in the degree of electronic interaction with the substrate. With the aim of reaching, also for CoTPP, a comprehensive view of molecular organization on Fe, we complement here our previous investigations by following the growth of the CoTPP film for increasing coverage, showing that an ordered stacking of such molecules is indeed realized at least up to four molecular layers.

1 Introduction

Ultra-thin molecular films grown on metallic substrates are currently employed for a variety of applications in the field of microelectronics, chemical sensing, protective coatings *etc.* [1,2]. They serve also as interesting model systems for fundamental research aimed at understanding the complex chemical, electronic and magnetic interactions occurring at their hybrid interface [3].

We have focused our experimental efforts on the technologically relevant Fe substrate, coupled to a special class of organic molecules, namely tetra-phenyl-porphyrins (TPP) [4]. Porphyrins are aromatic molecules composed by a ring (also called the macrocycle) of four pyrrole units, with their N atoms capable of binding a metallic ion in the centre of the ring. Four phenyl groups are then attached at the edges of the macrocycle, in the so-called meso positions [5]. This TPP molecular configuration allows the central ion to interact with the environment on both sides of the ring, and in particular with the Fe substrate, where those molecules can lie flat, thus maximizing the contact area and bringing the metal ion close to its very reactive surface.

Rather unexpectedly, we observed that a certain degree of molecular decoupling can be obtained on Fe(001) after passivating the surface with a single layer of oxygen. This was first demonstrated with ZnTPP molecules [6,7], characterized by a central ion with a completely filled 3*d* shell and therefore by a relatively low reactivity. At monolayer (ML) coverage, the electronic structure of ZnTPP is preserved and the molecules are free to arrange on the substrate by forming a commensurate (5 × 5) superstructure.

Our investigation was later extended to CoTPP, characterized by the presence of an unpaired electron on the Co ion, which increases the molecular reactivity and gives the molecule a non-zero magnetic moment [4]. As in the case of ZnTPP, we observe also for CoTPP the formation of a highly ordered molecular assembling at ML coverage, together with the absence of any strong chemical interaction with the oxygen-passivated surface [8]. As a consequence, the magnetic structure of CoTPP molecules in close contact with Fe is preserved, inducing even at room temperature a long-range magnetic ordering of the first CoTPP monolayer, as we documented in Ref. [9]. However, some differences in the packing configuration and in the electronic interaction with the substrate are observed with respect to the comparatively better investigated ZnTPP system [6,7].

With the aim of improving our knowledge of the CoTPP system, in the present communication we report, together with a brief overview of its peculiar characteristics at ML coverage, an in-depth analysis of CoTPP growth on oxygen-passivated Fe(001) for increasing thicknesses of the molecular film. Our investigation, performed with x-ray and UV photoemission spectroscopy techniques (XPS and UPS, respectively) complements the results of Refs. [8,9] and provide useful information on the CoTPP growth mode and on the spectroscopic signals recorded on thicker molecular layers.

* Corresponding author: alberto.calloni@polimi.it

2 Experimental details

The Fe(001) substrate was prepared by growing a thick (about 500 nm) Fe film on a MgO(001) crystal. The bare Fe surface was then passivated by dosing 30 L of molecular oxygen [1 langmuir (L) =$1 \cdot 10^{-6}$ Torr·s] at high temperature (450 °C) and subsequently annealing at 700 °C. The passivated surface shows a square arrangement of O atoms, in registry with the Fe lattice, giving rise to a $p(1 \times 1)$O superstructure [10,11]. CoTPP molecules were grown by means of Organic Molecular Beam Epitaxy (OMBE) in a dedicated vacuum chamber with a base pressure in the 10^{-10} Torr range. The deposition rate was calibrated by means of a quartz microbalance and was kept at the rather small value of about 0.5 ML per minute, where 1 ML corresponds to a thickness of 3.06 Å [12]. The CoTPP films were then transported *in-situ* to the analysis chamber through a specially designed system of interconnected vacuum chambers working at a base pressure in the low 10^{-10} Torr range [13].

XPS and UPS were performed by using Mg Kα (hν=1253.6 eV) and HeI (hν=21.2 eV) radiation, respectively, and by collecting the photoelectrons with a hemispherical electron analyser, providing an overall full width at half maximum (FWHM) energy resolution of 0.9 eV and 15 meV, respectively.

3 Results and discussion

Figure 1 shows a representative Low Energy Electron Diffraction (LEED) image acquired on a single layer of CoTPP molecules on Fe(001)-$p(1 \times 1)$O. The observed pattern is the superposition of two square arrangements of diffraction spots tilted by ±36.9° with respect to the substrate <100> directions (the reciprocal space schematic of Figure 1 helps visualizing the two square lattices). The diffraction spots observed on the Fe(001)-$p(1 \times 1)$O substrate (image not shown) are located in the position of large open symbols.

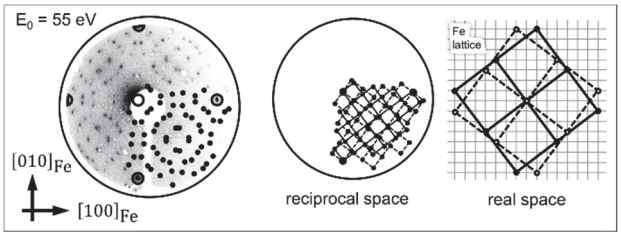

Fig. 1. LEED image for 1 ML of CoTPP on Fe(001)-$p(1 \times 1)$O. Diffraction spots are marked with dots (large open dots are representative of the diffraction pattern from the substrate). The two domains contributing to the overall signal from CoTPP molecules are sketched next to the LEED image, both in reciprocal and real space. In the latter case, a finer grid is superimposed to the CoTPP lattice, representative of the Fe(001) surface lattice.

The observed periodicity is compatible in real space with a square and commensurate disposition of molecules, spaced one with respect to the other 5 times the Fe(001) lattice parameter, *i.e.* about 1.4 nm. This inter-molecular distance is compatible with the planar dimensions of the TPP molecule, and is common also to the ZnTPP ML, even though in the latter case the molecular lattice is aligned with the Fe crystallographic directions [6].

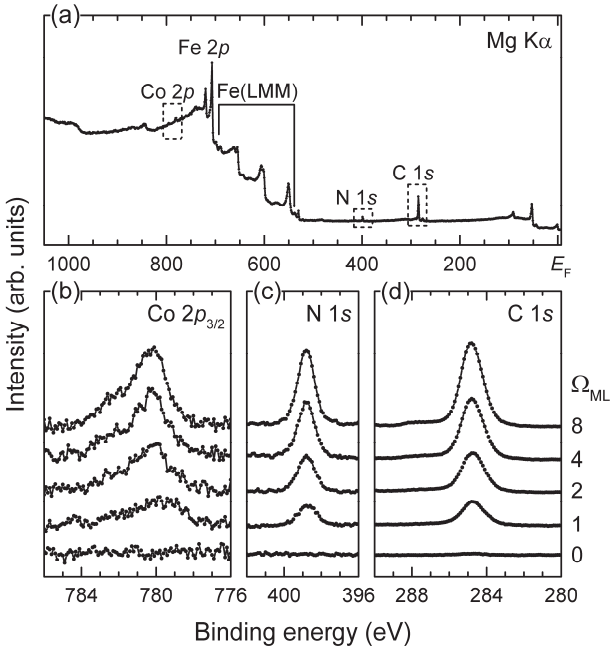

Fig. 2. (a) XPS wide scan (pass energy 40 eV) acquired on a 4 ML of CoTPP film. The Fe(LMM) label refers to the signal from Fe Auger electrons. (b-d) Detailed scans (pass energy 20 eV) acquired on CoTPP films of increasing thickness (Ω) from 0 to 8 ML. A linear background is subtracted to the experimental data of panel (b), accounting for the signal coming from the Fe 2*p* line located at lower BE [see panel (a)]. An integral (Shirley) background is subtracted in panels (c,d).

XPS results are shown in **Figure 2**. The wide scan of Figure 2a, related to a 4 ML CoTPP film, helps identifying the main spectroscopic signals from the hybrid system. The spectrum is dominated by the photoemission features from the Fe(001)-$p(1 \times 1)$O substrate: photoemission from Fe 2*p* orbitals at a binding energy (BE) of about 710 eV and Fe LMM Auger emission at lower energies (550-700 eV). Photoemission features from C, N and Co atoms from the CoTPP molecule, however, are clearly detected. The CoTPP layer stoichiometry is computed from the C 1*s*, N 1*s* and Co $2p_{3/2}$ signal intensities by correcting for the element- and transition- specific photoemission cross sections [14]. The retrieved C to Co and N to Co ratios, averaging the results obtained at larger coverages, are 47±5 and 4.0±0.5, respectively, in good agreement with the chemical composition of the CoTPP molecule (C:Co=44:1 and N:Co=4:1).

The detail scans of Figure 2b-d show the evolution with the film thickness (Ω) of the relevant photoemission features from the CoTPP molecule, after the subtraction of a proper background (see the caption of Figure 2 for further details). By comparing the spectra acquired on the thicker film with the ones of the first layer it is in principle possible to highlight changes in the chemical configuration of the related atomic species. In the present case, a shift towards lower BE is detected for the Co $2p_{3/2}$ feature, which can be attributed to a partial reduction of the Co ion resulting from the transfer of electronic charge

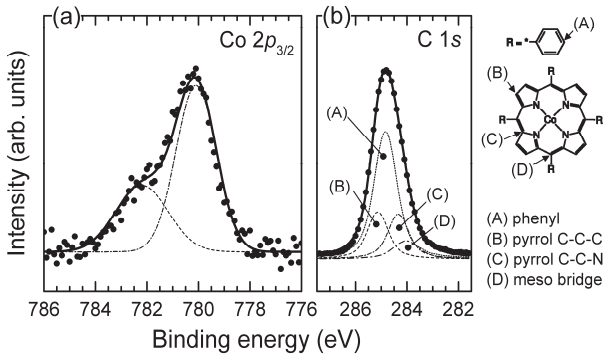

Fig. 3. Lineshape analysis of (a) the Co $2p_{3/2}$ spectrum and (b) the C 1*s* spectrum related to the 8 ML CoTPP film (see the caption of Fig. 2 for more details). A schematic is added illustrating the contribution of different C species to the overall C 1*s* lineshape.

from the substrate [8,15]. Interestingly, the other photoemission features show comparatively smaller BE shifts (about 0.1 eV), rather attributed to instrumental effects such as an enhanced screening of the photoemission hole by the Fe substrate [8]. This observation points out a preferential interaction between the substrate and the central CoTPP ion.

The analysis of the photoemission lineshapes is presented in **Figure 3** for a coverage of 8 ML. Co $2p_{3/2}$ photoemission is modelled in Figure 3a with the sum of two Voigt lineshapes located at a BE of 780.1 eV and 782.2 eV. The BE of the highest intensity peak is very close to the value usually reported for the Co^{2+} ion in inorganic compounds [16], in agreement with the oxidation state of the metal ion in TPP. According to Refs. [17,18] on the parent compound metal phtalocyanine, the presence of a double peak is not related to chemically inequivalent Co species, but rather to the coupling of the $2p_{3/2}$ photoemission core hole with the valence spin ***S***, resulting in a partial removal of the m_j degeneracy of the $2p_{3/2}$ orbital. The asymmetric shape of the Co $2p_{3/2}$ peak is therefore a fingerprint of the CoTPP molecule and is indicative of the presence of unpaired valence spins. This in turns is responsible for the magnetic activity of the molecule. We note that, even if shifted, the Co $2p_{3/2}$ signal retains its asymmetric lineshape at monolayer coverage. This is consistent with the long range magnetic order observed for the 1 ML CoTPP film [9]. The N 1*s* lineshape (not shown in Figure 3) is described by a single symmetric peak, consistent with the presence of chemically equivalent N species in the CoTPP molecule. Conversely, the C 1*s* lineshape of Figure 3b, peaking at 284.8 eV, is the sum of several Voigt lineshapes, each representing the contribution from specific C species: C atoms in phenyl groups, those interacting with one of the four N atoms in the pyrrole rings (pyrrol C-C-N), the remaining pyrrole carbons (pyrrol C-C-C) and the C atoms in meso-bridge positions. In the fit of Figure 3b, the relative BE positions of those C species are taken from Ref. [19] and fixed together with their peak intensity ratio (24:8:8:4) and width. The good quality of the resulting fit (which neglects the shake-up excitations at higher BE, visible in Figure 2 [20]) confirms the integrity of the

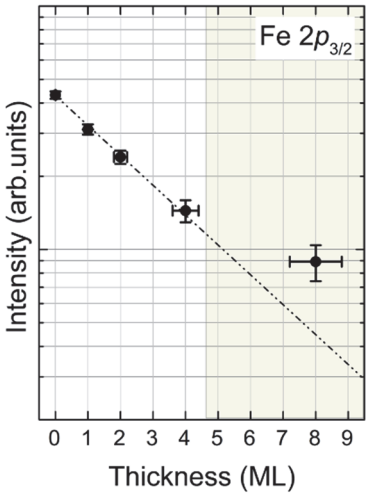

Fig. 4. Intensity of photoemission from the Fe $2p_{3/2}$ orbital as a function of the CoTPP layer thickness, plotted with a semi-logarithmic scale. The straight line describes the thickness evolution of the first four data points. A deviation from this linear trend is detected at larger coverages (grey area).

CoTPP molecular skeleton (including side groups) upon thermal evaporation and deposition on the Fe substrate.

Together with the spectra from CoTPP atomic species, we collected also the photoemission signal from the Fe $2p_{3/2}$ orbital. The intensity evolution of such signal with the molecular coverage is plotted in **Figure 4** with a semi-logarithmic scale. Up to a coverage of 4 ML the experimental points almost perfectly align along a straight line, a trend expected for an exponential attenuation of the substrate emission with the thickness of the overlayer, as in the case of a layer-by-layer growth. The experimental Fe $2p_{3/2}$ intensity for the 8 ML film deviates from the above trend, possibly due to the onset of molecular clustering. This assessment of a layer-by-layer growth of CoTPP molecules, at least at lower coverages, confirms the large degree of order characteristic of the CoTPP/ Fe(001)-$p(1 \times 1)$O system. However, this is not a foregone conclusion, considering the absence of any complementary information coming from other techniques such as LEED, where the diffraction pattern is observed to fade away above 1 ML. On the other hand, this behaviour is compatible with our previous near-edge x-ray adsorption fine structure spectroscopy (NEXAFS) results on the ZnTPP/ Fe(001)-$p(1 \times 1)$O system, placing the onset of ZnTPP deviation from a flat configuration (thus favouring molecular clustering) at about 4 ML [7]. The inelastic mean free path of Fe $2p_{3/2}$ electrons (λ_{Fe}), calculated from the linear regression of Figure 4, is about 1 nm, *i.e.* of the same order of magnitude, but slightly smaller, than value retrieved from predictive equations [21]. As discussed in Ref. [22], this is possibly related to a not negligible contribution from elastic scattering events to the attenuation of the photoelectron signal.

Finally, we provide some novel results about the electronic structure of CoTPP molecules at monolayer coverage, by using angle resolved UPS. **Figure 5** compares the spectra measured on the bare substrate (Figure 5a) with those of 1 ML CoTPP/

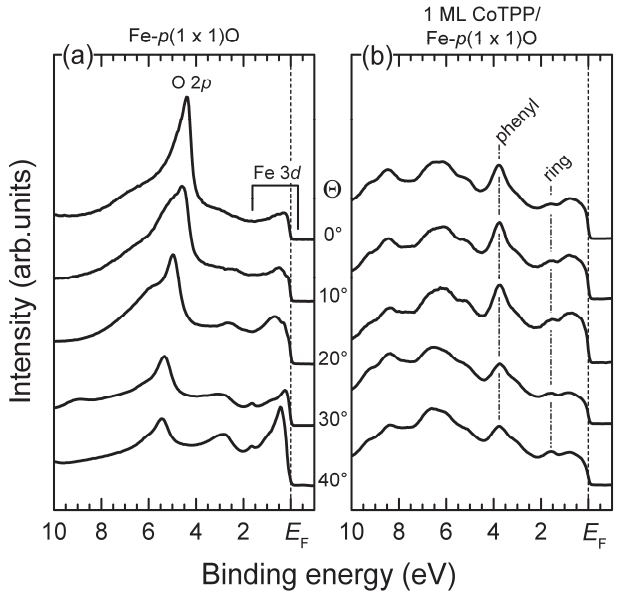

Fig. 5. Angle resolved UPS spectra from (a) Fe(001)-$p(1 \times 1)$O (adapted from Ref. [25]) and (b) 1 ML CoTPP on Fe(001)-$p(1 \times 1)$O. The spectra are collected by varying the polar angle of emission (Θ) from 0° (electron emitted along the surface normal) towards the $\overline{\Gamma X}$ direction of the surface Brillouin zone. The $\overline{X}$ point is reached for Θ≈30°.

Fe(001)-$p(1 \times 1)$O (Figure 5b) under the same experimental conditions, by increasing the polar angle (Θ) of electron emission along the $\overline{\Gamma X}$ direction of the surface Brillouin zone (SBZ). The substrate spectra are characterized by the presence of O 2*p* and Fe 3*d* features, at a BE in the 4.3 to 5.5 eV range and close to the Fermi energy (E_F), respectively. Both features show pronounced changes in their shape, intensity and energy position across the SBZ. Conversely, the spectra acquired on the CoTPP layer are all very similar, irrespective of the emission angle. Among the features associated to photoemission from CoTPP molecules, we recall the broad peak at 1.6 eV (3.8 eV) related to photoemission from the tetra-pyrrole ring (phenyl groups) [6,9]. Features at larger BE are alternatively assigned to the ring or phenyls. While photoemission from O 2*p* orbitals gives a nil contribution at 1 ML CoTPP coverage, the signal from Fe 3*d* states is not quenched. Even if in Ref. [8] we present evidence of an additional molecular state at a BE of 0.95 eV (not shown in Figure 5), the signal intensity close to E_F is largely related to photoemission from the substrate. Following our previous discussion on photoelectron attenuation through the CoTPP layer, and in line with recent literature studies on different hybrid molecular/metal interfaces [23,24], we explain the non-dispersing behaviour of metallic bulk states in the 1 ML CoTPP spectra by the contribution of elastic photoelectron scattering through the molecular layer.

4 Conclusions

The growth of CoTPP on the oxygen-passivated Fe(001) surface has been investigated by means of photoemission spectroscopy (XPS and UPS) for increasing CoTPP coverage. Our results show the formation of a highly ordered film at ML coverage, characterized by a well-defined diffraction pattern (investigated with LEED) and nearly unperturbed valence electronic states. At larger coverages, the present results concerning the attenuation of substrate photoelectrons from the molecular layer provide a strong evidence of a relatively ordered and layer-by-layer CoTPP growth, at least up to a coverage of 4 ML.

Authors are grateful to M. Finazzi, F. Carobene, M. Menegazzo, G. Merzoni and F. Zecchi (Dipartimento di Fisica, Politecnico di Milano) for useful discussions.

References

1. M. Cinchetti, V.A. Dediu, L.E. Hueso, Nat. Mater. **16**, 507 (2017)
2. L. Bartels, Nat. Chem. **2**, 87 (2010)
3. J. V. Barth, G. Costantini, K. Kern, Nature **437**, 671 (2005)
4. J.M. Gottfried, Surf. Sci. Rep. **70**, 259 (2015)
5. T. Wölfle, A. Görling, W. Hieringer, Phys. Chem. Chem. Phys. **10**, 5739 (2008)
6. G. Bussetti, A. Calloni, M. Celeri, R. Yivlialin, M. Finazzi, F. Bottegoni, L. Duò, F. Ciccacci, Appl. Surf. Sci. **390**, 856 (2016)
7. A. Picone, D. Giannotti, A. Brambilla, G. Bussetti, A. Calloni, R. Yivlialin, M. Finazzi, L. Duò, F. Ciccacci, A. Goldoni, A. Verdini, L. Floreano, Appl. Surf. Sci. **435**, 841 (2018)
8. A. Calloni, M.S. Jagadeesh, G. Bussetti, G. Fratesi, S. Achilli, A. Picone, A. Lodesani, A. Brambilla, C. Goletti, F. Ciccacci, L. Duò, M. Finazzi, A. Goldoni, A. Verdini, L. Floreano, Appl. Surf. Sci. ,144213 (2019)
9. M.S. Jagadeesh, A. Calloni, A. Brambilla, A. Picone, A. Lodesani, L. Duò, F. Ciccacci, M. Finazzi, G. Bussetti, Appl. Phys. Lett. **115**, 082404 (2019)
10. F. Donati, P. Sessi, S. Achilli, A. Li Bassi, M. Passoni, C.S. Casari, C.E. Bottani, A. Brambilla, A. Picone, M. Finazzi, L. Duò, M.I. Trioni, F. Ciccacci, Phys. Rev. B **79**, 195430 (2009)
11. A. Picone, A. Brambilla, A. Calloni, L. Duò, M. Finazzi, F. Ciccacci, Phys. Rev. B **83**, 235402 (2011)
12. C. Castellarin-Cudia, P. Borghetti, G. Di Santo, M. Fanetti, R. Larciprete, C. Cepek, P. Vilmercati, L. Sangaletti, A. Verdini, A. Cossaro, L. Floreano, A. Morgante, A. Goldoni, ChemPhysChem **11**, 2248 (2010)
13. G. Berti, A. Calloni, A. Brambilla, G. Bussetti, L. Duò, F. Ciccacci, Rev. Sci. Instrum. **85**, 073901 (2014)
14. J.J. Yeh, I. Lindau, At. Data Nucl. Data Tables **32**, 1 (1985)
15. T. Lukasczyk, K. Flechtner, L.R. Merte, N. Jux, F. Maier, J.M. Gottfried, H.-P. Steinrück, J.

Phys. Chem. C **111**, 3090 (2007)

16. M.C. Biesinger, B.P. Payne, A.P. Grosvenor, L.W.M. Lau, A.R. Gerson, R.S.C. Smart, Appl. Surf. Sci. **257**, 2717 (2011)
17. L. Massimi, M. Angelucci, P. Gargiani, M.G. Betti, S. Montoro, C. Mariani, J. Chem. Phys. **140**, 244704 (2014)
18. C. Isvoranu, B. Wang, K. Schulte, E. Ataman, J. Knudsen, J.N. Andersen, M.L. Bocquet, J. Schnadt, J. Phys. Condens. Matter **22**, 472002 (2010)
19. C.C. Cudia, P. Vilmercati, R. Larciprete, C. Cepek, G. Zampieri, L. Sangaletti, S. Pagliara, A. Verdini, A. Cossaro, L. Floreano, A. Morgante, L. Petaccia, S. Lizzit, C. Battocchio, G. Polzonetti, A. Goldoni, Surf. Sci. **600**, 4013 (2006)
20. C. Castellarin-Cudia, T. Caruso, E. Maccallini, A. Li Bassi, P. Carrozzo, O. De Luca, A. Goldoni, V. Lyamayev, K.C. Prince, F. Bondino, E. Magnano, R.G. Agostino, C.S. Casari, J. Phys. Chem. C **119**, 8671 (2015)
21. S. Tanuma, C.J. Powell, D.R. Penn, Surf. Interface Anal. **21**, 165 (1994)
22. T. Graber, F. Forster, A. Schöll, F. Reinert, Surf. Sci. **605**, 878 (2011)
23. J. Stöckl, A. Jurenkow, N. Großmann, M. Cinchetti, B. Stadtmüller, M. Aeschlimann, J. Phys. Chem. C **122**, 6585 (2018)
24. L. Giovanelli, F.C. Bocquet, P. Amsalem, H.-L. Lee, M. Abel, S. Clair, M. Koudia, T. Faury, L. Petaccia, D. Topwal, E. Salomon, T. Angot, A.A. Cafolla, N. Koch, L. Porte, A. Goldoni, J.-M. Themlin, Phys. Rev. B **87**, 035413 (2013)
25. A. Calloni, G. Fratesi, S. Achilli, G. Berti, G. Bussetti, A. Picone, A. Brambilla, P. Folegati, F. Ciccacci, L. Duò, Phys. Rev. B **96**, 085427 (2017)